

Linköping University Post Print

The role of aluminum oxide buffer layer in organic spin-valves performance

Yiqiang Zhan, Xianjie Liu, Elin Carlegrim, Fenghong Li, I Bergenti, P Graziosi,
V Dediu and Mats Fahlman

N.B.: When citing this work, cite the original article.

Original Publication:

Yiqiang Zhan, Xianjie Liu, Elin Carlegrim, Fenghong Li, I Bergenti, P Graziosi, V Dediu and Mats Fahlman, The role of aluminum oxide buffer layer in organic spin-valves performance, 2009, APPLIED PHYSICS LETTERS, (94), 5, 053301.

<http://dx.doi.org/10.1063/1.3078274>

Copyright: American Institute of Physics

<http://www.aip.org/>

Postprint available at: Linköping University Electronic Press

<http://urn.kb.se/resolve?urn=urn:nbn:se:liu:diva-16980>

The role of aluminum oxide buffer layer in organic spin-valves performance

Y. Q. Zhan,^{1,a)} X. J. Liu,¹ E. Carlegrim,¹ F. H. Li,¹ I. Bergenti,² P. Graziosi,² V. Dediu,² and M. Fahlman¹

¹Department of Physics, Chemistry and Biology, Linköping University, S-581 83 Linköping, Sweden

²Istituto per lo Studio di Materiali Nanostrutturati, Consiglio Nazionale delle Ricerche, ISMN-CNR, via Gobetti 101, 40129 Bologna, Italy

(Received 12 December 2008; accepted 8 January 2009; published online 2 February 2009)

The electronic structures of the 8-hydroxyquinoline-aluminum (Alq₃)/Al₂O₃/Co interfaces were studied by photoelectron spectroscopy. A strong interface dipole was observed, which leads to a reduction in the electron injection barrier. The x-ray photoelectron spectroscopy spectra further indicate that the Al₂O₃ buffer layer prevents the chemical interaction between Alq₃ molecules and Co atoms. X-ray magnetic circular dichroism results demonstrate that a Co layer deposited on an Al₂O₃ buffered Alq₃ layer shows better magnetic ordering in the interface region than directly deposited Co, which suggests a better performance of spin valves with such a buffer layer. This is consistent with the recent results from [Dediu *et al.*, Phys. Rev. B **78**, 115203 (2008)]. © 2009 American Institute of Physics. [DOI: 10.1063/1.3078274]

Spin injection and transport in organic semiconductors have been gathering much attention since the demonstration of the magnetoresistive effects in lateral devices¹ and the spin valve (SV) effect in vertical devices.² One of the main issues in the vertical architecture of SVs is the quality of the top ferromagnetic (FM) electrode that is deposited on the organic film. For example, in the device discussed in Ref. 2, the Co electrode was deposited on top of 8-hydroxyquinoline aluminum (Alq₃) layer. It is well known that the FM properties of the top layer very much depend on the roughness of the substrate,^{3,4} and of course the interaction with the substrate as well. It has been frequently reported that the roughness of organic surface is rather high,^{4,5} which would affect the quality of FM electrode above it. Furthermore, our recent results⁶ have shown that Co atoms (or clusters) penetrate into the Alq₃ layer upon vapor deposition. The penetrated Co atoms and the Co atoms at the interface will chemical react with Alq₃ molecules.⁶ Not only does this chemical interaction create uncertainty in terms of how (and if) it affects the spin injection, but also the quality of Co film itself is crucially related to the interface.⁴ In conventional organic electronics, inserting a buffer layer in between the top electrode and the organic layer⁷⁻⁹ has been widely adopted to improve device performance. Following this approach, an organic SV with a thin layer of aluminum oxide inserted between the organic and top electrode recently has been demonstrated showing improved SV behavior.¹⁰

In this letter, ultraviolet and x-ray photoelectron spectroscopy (UPS and XPS) results on Co/Al₂O₃/Alq₃ interfaces are reported in comparison with the Co/Alq₃ interface. The energy level alignment at the Co/Al₂O₃/Alq₃ interfaces is discussed as well. Reasons for the improvement of the Co electrode upon inclusion of an Al₂O₃ buffer layer are presented based on our XPS and x-ray magnetic circular dichroism (XMCD) results.

The experiments were carried out using a Scienta® ESCA 200 spectrometer. The vacuum system consists of an analysis chamber and a preparation chamber. XPS and UPS

were performed in the analysis chamber at a base pressure of 10⁻¹⁰ mbar, using monochromatized Al(Kα) x-rays at $h\nu=1486.6$ eV and He I radiation at $h\nu=21.2$ eV, respectively. The experimental conditions were such that the full width at half maximum of the Au 4f_{7/2} line was 0.65 eV. The binding energies were obtained referenced to the Fermi level with an error of ± 0.1 eV. Sputtering and material depositions were done in a preparation chamber with a base pressure of 10⁻¹⁰ mbar. The Alq₃ was purchased from Sigma-Aldrich. Alq₃ was deposited *in situ* from a simple Knudsen cell with a flux rate of about 5 Å/min (estimated from the attenuation of the core level signals of the bottom layer). Co was deposited using a UHV e-beam evaporator (Omicron EFM3) at a deposition rate of about 3 Å/min. The aluminum oxide layer was deposited *ex situ* directly by channel spark method.¹¹ In order to investigate the buried Co/Al₂O₃/Alq₃ interface, first a 15 nm thick Alq₃ film was deposited on a sputter-cleaned Si-substrate, followed by deposition of about 2 nm Al₂O₃ buffer layer and 20 nm Co. Afterward, the sample was take out from vacuum and a simple *ex situ* peel-off technique was adopted to turn over the sample. A clean Si-substrate attached to a two-sided UHV-compatible conductive carbon tape was pressed onto the Co/Al₂O₃/Alq₃/Si sample in atmosphere. After separating the two Si-substrates, the Co/Al₂O₃/Alq₃ sample was peeled off from the Si-substrate and attached to the carbon tape. More detailed information of the peel-off technique can be found in Ref. 6. The inverted sample, now Alq₃/Al₂O₃/Co/tape, was transferred back into vacuum and analyzed by XPS (also angle-resolved XPS) and UPS. The inverted Alq₃/Co was made in the same way for comparison. The take-off angle noted in the figure is defined as the angle between the direction of the detected electrons and the surface of the sample, i.e., a 90° take-off angle means that the electrons are detected leaving perpendicular to the surface (parallel to the surface normal).

X-ray absorption spectroscopy (XAS) and XMCD measurements were performed at beamline D1011 of the MAX-II storage ring, located at the MAX-Laboratory for Synchrotron Radiation Research in Lund, Sweden. For both the XAS and XMCD measurements, the angle of incidence

^{a)}Electronic mail: yiqzh@ifm.liu.se.

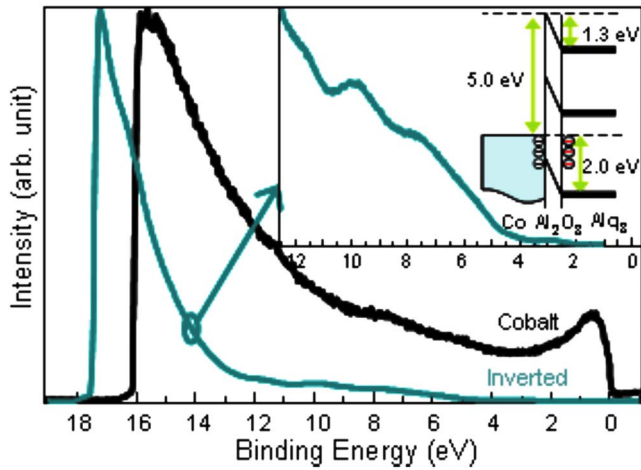


FIG. 1. (Color online) UPS spectra of the inverted $\text{Alq}_3/\text{Al}_2\text{O}_3/\text{Co}$ interface and pure Co. Inset: the enlarged valence band and energy band diagram of the $\text{Alq}_3/\text{Al}_2\text{O}_3/\text{Co}$ interface.

of the photon beam was set to 75° relative to the sample normal. For XMCD, the in-plane magnetization of the Co films was set by applying a magnetic field pulse of about 500 G. The XMCD spectra were recorded with a fixed helicity of the light and opposite magnetization directions.

The UPS spectra of both $\text{Alq}_3/\text{Al}_2\text{O}_3/\text{Co}$ and pure Co are shown in Fig. 1, denoted as “inverted” and “cobalt,” respectively. It can be clearly seen that the work function of the inverted structure, $\text{Alq}_3/\text{Al}_2\text{O}_3/\text{Co}$, is 3.7 eV, as estimated from the secondary electron cutoff, while the work function of the as-deposited Co film was deduced as 5.0 eV, which is in good agreement with previously published value.¹² In the inset of Fig. 1, the Alq_3 features clearly are present in the UPS spectrum of the inverted sample in the range of 2–13 eV, although there is an overlap with the tail of the huge secondary electron cutoff for the higher energies. The value of the highest occupied molecular orbital (HOMO) onset is 2.0 eV higher than the zero point, where the Fermi edge of pure Co sits.

From the data obtained from inverted structure ($\text{Alq}_3/\text{Al}_2\text{O}_3/\text{Co}$), the energy level alignment at the interface of Co-on- Al_2O_3 -covered- Alq_3 can be constructed as shown in inset of Fig. 1. Since the onset of Alq_3 HOMO is 2.0 eV below the Fermi level and the secondary electron cutoff is 3.7 eV below the vacuum level, the ionization potential can be deduced as 5.7 eV, which is consistent with previous values.^{6,13} The work function of Co is 5.0 eV, so the vacuum level offset at the interface between Alq_3 and Co is 1.3 eV, obtained by subtracting the work function of the inverted sample $\text{Alq}_3/\text{Al}_2\text{O}_3/\text{Co}$ (3.7 eV) from that of Co. This offset, caused by a strong interface dipole, rigidly shifts the valence features of Alq_3 toward higher binding energy, increasing the hole-injection barrier and decreasing the electron-injection barrier compared to the case of vacuum level alignment to a 5.0 eV work function electrode. A similarly sized dipole-induced vacuum level offset (1.4 eV) was found at the Co-on- Alq_3 interface.⁶

In addition to the above described energy level alignment, the XPS core level spectra of both Alq_3 and Co were measured to study the differences between the Alq_3/Co interface with and without Al_2O_3 buffer layer. Figure 2 describes the $\text{O}(1s)$ spectra of the inverted Alq_3/Co and

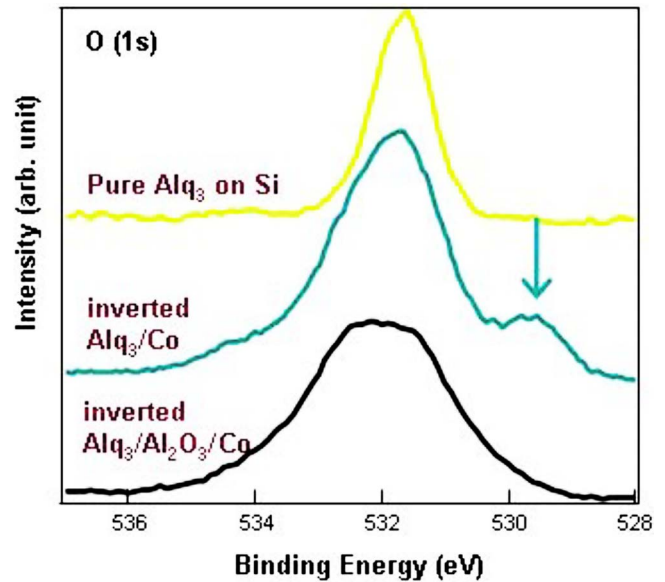


FIG. 2. (Color online) Photoelectron spectra of $\text{O}(1s)$ of inverted $\text{Alq}_3/\text{Al}_2\text{O}_3/\text{Co}$ and Alq_3/Co interfaces and Alq_3 film.

$\text{Alq}_3/\text{Al}_2\text{O}_3/\text{Co}$, where the $\text{O}(1s)$ spectrum of pure Alq_3 is shown as a reference. The appearance of an additional peak (529.6 eV) in the inverted Alq_3/Co system has been ascribed to a strong interaction between Co and the phenoxide part of Alq_3 .⁶ This additional peak disappears when the Al_2O_3 buffer layer is inserted between Alq_3 and Co. There is only one peak in the spectrum of $\text{O}(1s)$, which matches very the peak of the pure Alq_3 .

The angle dependent $\text{Co}(2p)_{3/2}$ XPS spectra of both the Alq_3 and Co interfaces with and without an Al_2O_3 buffer layer are shown in the top and bottom parts of Fig. 3, respectively. The $\text{Co}(2p)_{3/2}$ XPS spectra measured with different takeoff angles are denoted as the values of the angles. In the Alq_3/Co system, a clear new peak appeared at the position of 781 eV.⁶ When decreasing the takeoff angle, the ratio between this peak and the main peak (778 eV) increased, which indicates that an interaction between Alq_3 and Co occurred at the interface. However, in the $\text{Alq}_3/\text{Al}_2\text{O}_3/\text{Co}$ system, as shown in the bottom part of Fig. 3, all the spectra have the

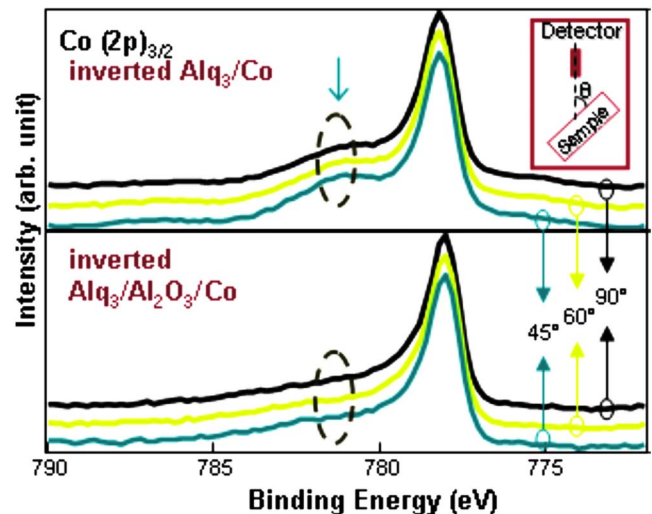


FIG. 3. (Color online) Angle-resolved photoelectron spectra of $\text{Co}(2p)_{3/2}$ at the inverted $\text{Alq}_3/\text{Al}_2\text{O}_3/\text{Co}$ and Alq_3/Co interfaces.

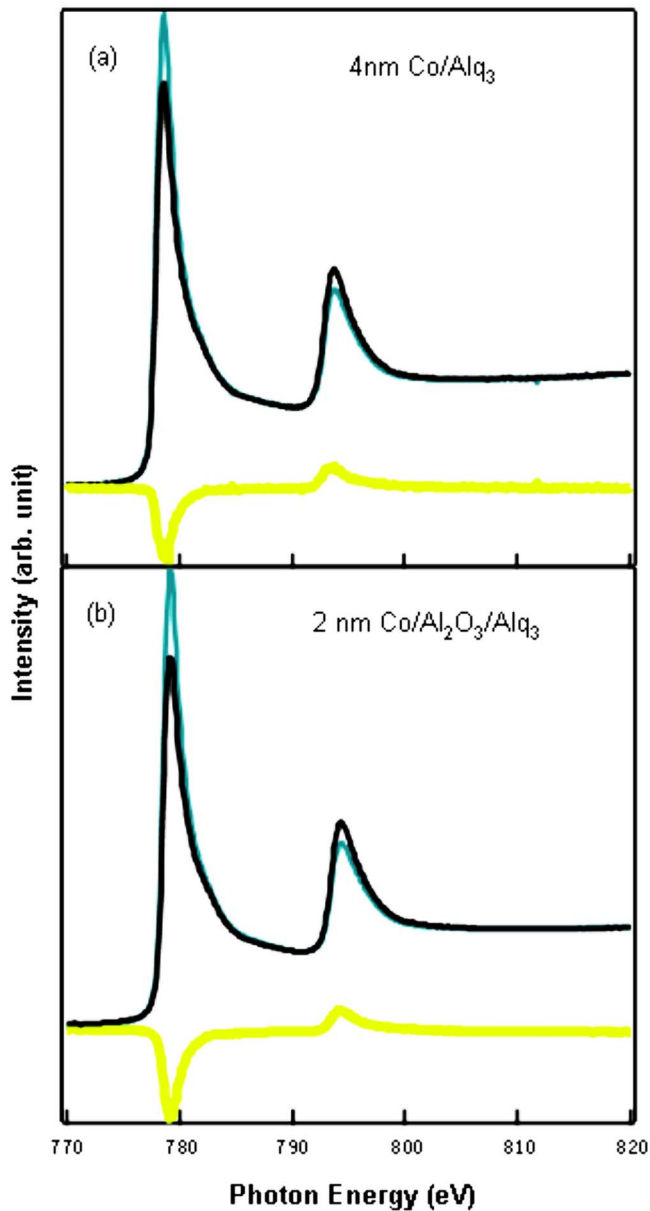


FIG. 4. (Color online) The XAS and XMCD curves of Co films. (a) 4 nm Co on top of bared Alq₃ film and (b) 2 nm Co on top of Al₂O₃ buffered Alq₃ film.

same feature independent upon the takeoff angles. There is no additional peak presented in the Co(2*p*)_{3/2} spectra, even at low takeoff angles. The absence of the new peak indicates the inserted Al₂O₃ buffer layer separates the Alq₃ and Co and prevents chemical interaction between them.

The Co *L*-edge XMCD measurements of Co deposited on bare Alq₃ and Al₂O₃ buffered Alq₃ were performed to determine the minimum Co thickness that starts to be FM in each case. Thickness of the Co film was increased step by step and the Co *L*-edge XMCD spectra was monitored *in situ* after each step at room temperature. The XMCD curves were obtained by taking the difference between the XAS spectra with in-plane magnetization parallel and antiparallel to the helicity of the circularly polarized light. Figure 4(a) shows the XMCD curve obtained from a 4 nm Co film on top of

Alq₃ and related XAS spectra. Before reaching this thickness, no XMCD signal was detected.

However, in the case of depositing Co on Al₂O₃/Alq₃, the minimum thickness reduced to 2nm. As shown in Fig. 4(b), the XMCD signal of 2nm Co on top of Al₂O₃/Alq₃ is as strong as the one for two times thicker Co on Alq₃. It is interesting to note that the direct contact Alq₃-based vertical SVs without buffer layer do not show any SV effect at room temperature,² but buffered vertical SVs do.¹⁰ Although the authors suggested the improvement on the room-temperature operation efficiency might be due to the enhancement of the room-temperature surface magnetization in La_{0.7}Sr_{0.3}MnO₃ (LSMO). Here, our XMCD results provide another possible reason for the success of Alq₃-based buffered SVs room temperature operation. In the direct device, a Co layer of about 3.5 nm thickness at the interface region is not FM at room temperature so it probably will act as a spin scattering layer rather than contribute as a spin injector. However, there is only less than 2 nm thickness of such a nonferromagnetic Co layer in the buffered device. The latter thickness is reasonably close to that of intermixed region in Alq₃/Al₂O₃/Co.⁶

The electronic structure of the Co/Al₂O₃/Alq₃ interface was investigated by means of photoelectron spectroscopy. An interfacial dipole of about 1.3 eV was observed in a direction that results in a shift of the whole energy levels of the Alq₃ over layer to higher binding energies with respect to the Fermi level. The core-level XPS spectra of both Alq₃ and Co indicate that the interaction between Co and Alq₃ can be prevented by inserting an Al₂O₃ buffer layer. Furthermore, the XMCD measurements confirm that the Co film deposited on top of Al₂O₃ buffered has better quality than the one on bare Alq₃. This high quality Co layer gives the possibility of operation of buffered vertical SVs at room temperature.

¹V. Dediu, M. Murgia, F. C. Maticotta, C. Taliani, and S. Barbanera, *Solid State Commun.* **122**, 181 (2002).

²Z. H. Xiong, D. Wu, Z. Vally Vardeny, and J. Shi, *Nature (London)* **427**, 821 (2004).

³S. J. Steinmuller, C. A. F. Vaz, V. Strom, C. Moutafis, D. H. Y. Tse, C. M. Gurtler, M. Klau, J. A. C. Bland, and Z. Cui, *Phys. Rev. B* **76**, 054429 (2007).

⁴I. Bergenti, A. Riminucci, E. Arisi, M. Murgia, M. Cavallini, M. Solzi, F. Casoli, and V. Dediu, *J. Magn. Magn. Mater.* **316**, e987 (2007).

⁵F. Zhang, Z. Xu, D. Zhao, S. Zhao, W. Jiang, G. Yuan, D. Song, Y. Wang, and X. Xu, *J. Phys. D* **40**, 4485 (2007).

⁶Y. Q. Zhan, M. P. de Jong, F. H. Li, V. Dediu, M. Fahlman, and W. R. Salaneck, *Phys. Rev. B* **78**, 045208 (2008).

⁷L. S. Hung, C. W. Tang, and M. G. Mason, *Appl. Phys. Lett.* **70**, 152 (1997).

⁸Y. Q. Zhan, Z. H. Xiong, H. Z. Shi, S. T. Zhang, Z. Xu, G. Y. Zhong, J. He, J. M. Zhao, Z. J. Wang, E. Obbard, H. J. Ding, X. J. Wang, X. M. Ding, W. Huang, and X. Y. Hou, *Appl. Phys. Lett.* **83**, 1656 (2003).

⁹S. T. Zhang, Y. C. Zhou, J. M. Zhao, Y. Q. Zhan, Z. J. Wang, Y. Wu, X. M. Ding, and X. Y. Hou, *Appl. Phys. Lett.* **89**, 043502 (2006).

¹⁰V. Dediu, L. E. Hueso, I. Bergenti, A. Riminucci, F. Borgatti, P. Graziosi, C. Newby, F. Casoli, M. P. De Jong, C. Taliani, and Y. Zhan, **78**, 115203 (2008).

¹¹V. A. Dediu, J. López, F. C. Maticotta, P. Nozar, G. Ruani, R. Zamboni, and C. Taliani, *Phys. Status Solidi B* **215**, 625 (1999).

¹²A. N. Caruso, D. L. Schulz, and P. A. Dowben, *Chem. Phys. Lett.* **413**, 321 (2005).

¹³S. T. Lee, X. Y. Hou, M. G. Mason, and C. W. Tang, *Appl. Phys. Lett.* **72**, 1593 (1998).